

# Proceedings of the Institute of Acoustics

## TIME AND FREQUENCY DOMAIN ANALYSIS OF RESONANT SCATTERING BY FLUID LOADED SPHERES

Peter D Thome (1)(2), Terry J Brudner (1) & Kendall R Waters (1)

(1) Applied Research Laboratories, The University of Texas at Austin, P.O. Box 8029, Austin, Texas 78713-8029.

(2) Work conducted while visiting ARL:UT. Present address the Proudman Oceanographic Laboratory, Bidston Observatory, Birkenhead, Merseyside, L43 7RA, UK.

### ABSTRACT

In recent years the application of resonance scattering theory, RST, has provided a description of the scattering process which has yielded valuable insight into the mechanisms of scattering. The RST approach resolves the scattered signal into two components; a background and a resonant term. In the present study the RST approach is employed in an examination of the backscattered echo from spheres in the time and frequency domain, and the detailed structure of the background and resonant components of the backscattered signal are examined in both domains. To achieve this comparison a linear frequency modulated signal has been employed. Using a linear system Fourier analysis approach, pulse compression has been applied to the signal and this has allowed measurements to be taken in the time domain, which readily show the component nature of the backscattered echo. Using the time data, sections of the record have been separately transformed to obtain in the frequency domain the constituent background and resonant form functions. Further, time frequency plots have been generated to examine the association between the time domain echo and the form function structure. To compare these observations with predictions, the RST description of sphere scattering has been coupled with the spectrum of the insonifying signal to predict, both in the time and frequency domain, the character of the backscattered echo.

### 1. INTRODUCTION

The scattering of underwater sound by elastic bodies of symmetry is a continuing area of study [1-4]. To understand the details of the scattering process it has become usual over the past decade to formulate the scattering problem in terms of resonant scattering theory [5-8], RST. The RST formulation characterises the form function structure in terms of the interference between a signal associated with a scattered background component and radiating surface eigen waves on the body stimulated by the incoming acoustic wave.

Until relatively recently the analysis of data scattered by spheroids and cylinders has principally focused on the frequency domain and the backscattered form function. Even in recent years where broadband pulse techniques have been applied, the analysis [9-15] has usually remained in the frequency domain, and comparisons with RST predictions have primarily focused on the location of the resonance frequencies. There have been studies conducted in the time domain [16-17], although these are scant compared with the frequency domain, and the application of RST in the time domain has been limited.

In the present study the resonant scattering approach is applied both in the time and frequency domain with particular attention paid to resolving the component structure of the time series echo and the underlying constituents of the form function structure. To achieve this experimentally a calibrated

## SPHERE RESONANT SCATTERING

broadband system employing a linear frequency modulated signal, LFM, or chirp was used to insonify spheres of different radius. Using pulse compression the duration of the chirp was reduced by approximately two orders of magnitude. This approach provided sufficient resolution in the time domain for the echo to be resolved into the background and resonant components, and this has allowed the composite structure of the form function to be analyzed. In the frequency domain not only are the locations of the resonant frequencies identified, but because the system is fully calibrated the entire background and resonant form function structure can be compared with predictions. Also because data is available in both domains, a time-frequency representation has been investigated.

### 2. ACOUSTIC ANALYSIS

For a broadband pulse incident upon a target the scattered signal can be expressed as,

$$p(\tau) = \frac{a}{2r} \int_{-\infty}^{\infty} f_{\infty}(x) e^{-ikx} dx \quad (1a)$$

$$h(x) = \int_{-\infty}^{\infty} p_f(\tau) e^{ikx} d\tau \quad (1b)$$

where the non-dimensional variables used in the calculations are

$$x = ka - \tau = \frac{ct}{2\pi a}$$

and  $f_{\infty}$  is the far field form function, which for sphere backscattering can be expressed as

$$f_{\infty} = \frac{2}{ix} \sum_{n=0}^{\infty} (-1)^n (2n+1) b_n \quad (2)$$

Here  $p_f(\tau)$  is the incident waveform,  $h(x)$  is its transform and  $r$  is the range from the sphere to the receiver.  $x=ka$ ,  $k$  is the wave number in the fluid and  $a$  is the sphere radius.  $b_n$  is composed of spherical Bessel and Hankel functions and their derivatives [7].

As mentioned, when considering the form function characteristics, the basis of the RST approach is to identify the background scattered signal and the resonance response which is associated with the modes of vibration of the sphere. For a solid sphere the background component is normally associated with the response of a rigid sphere. In the present work a slightly different background to the usual rigid component is employed. The rigid component contains both the specular return from the sphere and a diffracted wave. Experimentally the specular component is readily identified. However, the diffracted wave is less easily distinguished because of the sound radiated by the surface waves on the sphere. Therefore the specular reflection has been coherently subtracted from the full form function. This

## SPHERE RESONANT SCATTERING

approach yields a background and resonant component which can be directly compared with the observations. The resonant component is now defined as,

$$f_{-}^{res} = \left[ \frac{2}{ix} \sum_{n=-\infty}^{\infty} (-1)^n (2n+1) b_n \right] - f_{-}^{spec} \quad (3)$$

The specular component for the form function can be expressed as [18]

$$f_{-}^{spec} = Re^{-2ix} \quad (4)$$

For the case of  $x \gg 1$  the value for  $R_0 = (\rho_s c_s - \rho c) / (\rho_s c_s + \rho c)$  and the magnitude of the specular form function simply becomes the plane wave reflection coefficient. For the case of  $x \leq 5$  the expression is inaccurate and the specular echo was then obtained numerically by using the time domain solution for a rigid sphere, windowing the specular echo, transforming this component and multiplying by the reflection coefficient to give the response in the frequency domain.

### 3. EXPERIMENTAL ARRANGEMENT

Backscattering measurements were taken using stainless steel spheres suspended 1.5m above an upward looking adjacent source and receiver. The transceiver arrangement consisted of a rectangular 150kHz resonant array with a separate PVDF receiver. For the sphere scattering measurements the acoustic centres of the source and receiver subtended an angle of  $2^\circ$  to the sphere. Calculations of the form function for a sphere showed this marginal departure from the backscatter direction was not significant. For the observations a chirp was transmitted, this had a typical duration close to 1ms and swept between approximately 30-300kHz. The backscattered echoes from the spheres were digitised and stored. To obtain the impulse solution from the signal backscattered from the sphere, the inverse Fourier transform of the sphere transform function, to an impulse needed to be obtained. The measured spectrum of the backscattered signal,  $V_s(f)$ , was given by,

$$V_s(f) = C(f) \cdot H(f) \cdot S(f) \quad (5)$$

where  $C(f)$ ,  $H(f)$  and  $S(f)$  are the chirp, system and sphere frequency response respectively. To calibrate the response of the system, measurements of normal incidence reflections from the water-air interface were taken. These were simply obtained by removing the sphere. Such measurements were taken with each scattering data set. Assuming the water surface response to be uniform, the surface reflected spectrum,  $V_w(f)$ , is given by,

$$V_w(f) = C(f) \cdot H(f) \quad (6)$$

The band limited impulse response was acquired by coherently taking the ratio of the backscattered and water surface reflected spectra, this is equivalent to matched filtering,

## SPHERE RESONANT SCATTERING

$$V_s(\omega)/V_w(\omega) = S(\omega) \quad (7)$$

which is the sphere transform function, the inverse Fourier transform of this ratio provides the impulse response for the sphere. In forming the ratio due regard was taken of the phase change at the air-water interface. This approach reduced the pulse duration from 1ms to 10 $\mu$ s and allowed the temporal structure of the echo to be investigated. The advantage of using a long chirp signal over a short impulsive signal is a significant increase in the transmitted energy, which can be used to improve the signal to noise, and the amplitude of the spectrum is relatively uniform. All signals were also coherently averaged over repeated transmission to afford further noise rejection.

The spheres used in the experiments were stainless steel and had a radius of 0.873cm and 2.858cm. This allowed measurements to be taken over the range  $x=2-30$ . For the theoretical calculations the density, compressional and shear wave velocities for the spheres were respectively taken to be; 7930kgm<sup>-3</sup>, 5980ms<sup>-1</sup> and 3350ms<sup>-1</sup>. The water density and sound speed were taken to be 1000kgm<sup>-3</sup> and 1489ms<sup>-1</sup>.

### 4. RESULTS

#### 4.1 Time domain

The results obtained are displayed in figure 1. The data show time series for 0.873cm and 2.858cm spheres. For the smaller sphere it is difficult to resolve a discernable pattern in the waveform. There is the appearance of a large initial transient, although not particularly clear, followed by a relatively long tail, which slowly decays in time and has no obvious recognisable features. For the larger sphere the data is seen to be quite different. There is an evident structure in the time series consisting of a number of readily identifiable individual transient events superimposed upon a low level signal oscillation.

To compare predictions with the data collected the form function was computed in the frequency domain and the product of this with the Fourier transform of the incident impulse was inverse Fourier transformed to provide the time series response. This was conducted separately for the resonant and specular components using equations (3) and (4) respectively. This provided the components of the time series response, for a band limited impulse insonifying a sphere. The results of the calculations for the specular and the resonant echoes are compared with the data in figure 1a and 1b. The prediction for the specular echo is given by the thick line and the surface wave radiation component shown by the fine line.

Although experimentally for the smaller sphere it is difficult to distinguish definitive structures in the time series echo, the theoretical curve readily identifies the initial maximum amplitude return as due to the specular component and the decay tail as correspondingly associated with the surface wave radiation. The lack of form to the decay tail is due to the time duration of the insonifying pulse being greater than the travel time for the circumferential waves to travel the circumference of the sphere.

## SPHERE RESONANT SCATTERING

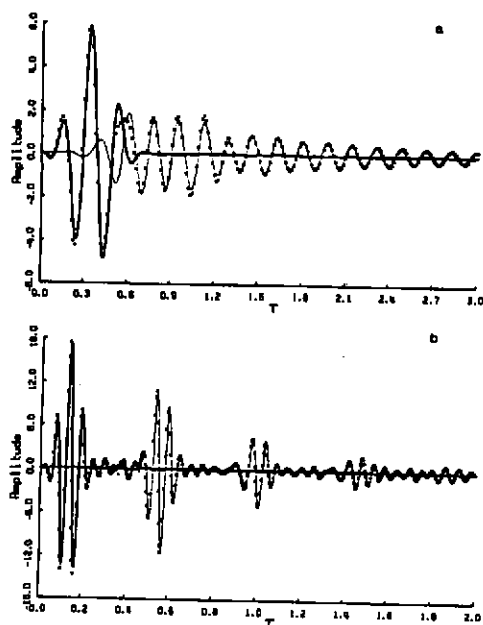


Fig.1. Backscattering of the compressed pulse from a) 0.873cm and b) 2.835cm radius spheres. x Measured. - Specular component from equation (1) and (4). - Resonance component from equation (1) and (3).

For the larger sphere the first transient echo is readily associated with the specular return. The prediction for the amplitude and duration of this component is in excellent agreement with the data. The first echo is associated with a reflection due to the impedance mismatch between the fluid and the sphere. The following series of pulses, which are readily identifiable, can be seen to arise from the surface wave propagation component on the sphere. This component is dominated in the present case by Rayleigh waves. These are identified with sound entering the sphere at the critical angle and launching two surface waves which propagate in opposite directions around the sphere. During circumnavigations of the surface sound radiation is continually taking place and the surface waves are gradually decreasing in magnitude. The other background echoes seen are considered to be caused by other creeping waves such as Franz and Whispering Gallery waves which contribute to the total backscattered signal. The time series is therefore dominated by a specular echo followed by a series of pulses which gradually reduce in amplitude with time due to radiation damping. As can be seen the comparison of the predictions with the data is excellent, with the observations and calculations for the dominant characteristics of the specular and Rayleigh components of the signal comparing favourably both in amplitude and time. Also

## SPHERE RESONANT SCATTERING

the general background features of the signal seem to be well replicated. The time domain analysis therefore provides an accurate description of structure of the backscattered echo, with the theoretical separation of the signal into its specular and resonant constituents allowing for a ready interpretation of the time domain signal in a manner similar to the interpretation of the form function.

### 4.2 Frequency domain

As shown in figure 1 the present data set readily allows the backscattered time series echo from the spheres to be separated into constituent elements due to a reflection from the sphere and the radiation ascribed to surface wave propagation. Figures 2 and 3 shows results for, (a), the standard form function,  $f_{\text{std}}$ , (b), the specularly reflected form function,  $f_{\text{spec}}$  and (c), the resonant form function,  $f_{\text{res}}$ , for the two spheres. These were obtained by respectively Fourier transforming the total time domain signal, the specular echo and the non-specular return respectively.

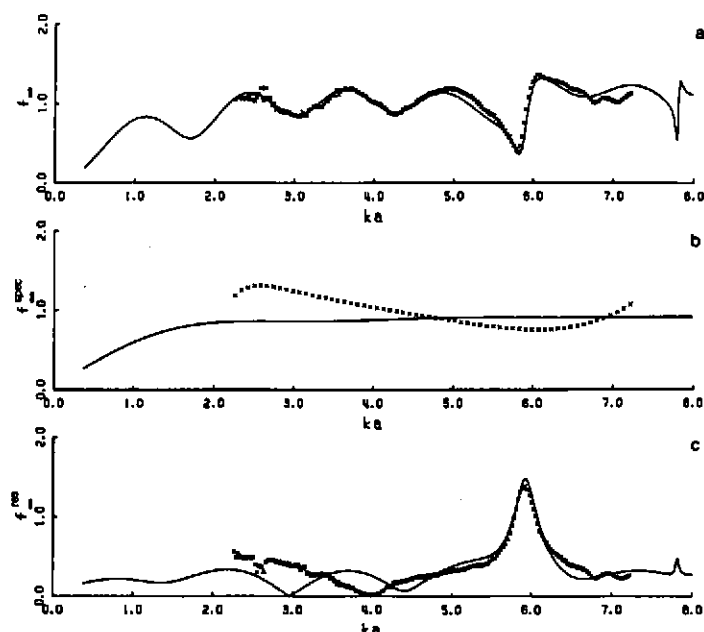


Fig.2. Comparison of the observed and predicted, a) Form function, b) Specular form function, and c) Resonance form function, for spheres of radius 0.873cm. - Theory a) equation (2), b) equation (4) and c) equation (3).

SPHERE RESONANT SCATTERING

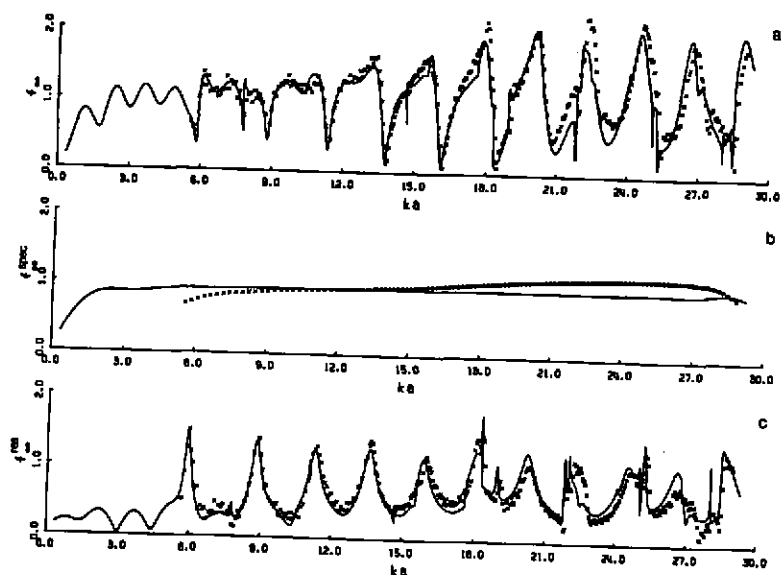


Fig.3. Comparison of the observed and predicted, a) Form function, b) Specular form function, and c) Resonance form function, for spheres of radius 2.858cm. - Theory a) equation (2), b) equation (4) and c) equation (3).

The standard form function data shows the usual structure which is generally observed when insonifying a metallic sphere acoustically. The observations exhibit an oscillatory variation in the form function up to an approximate value of  $x=5$  which is associated with diffraction. Above this  $x$  value there are large variations in the form function and these are due principally to the interference between the specular reflection and the Rayleigh wave resonances. Comparison of predictions with the observations shows good agreement, with the detailed structure of the form function being well represented theoretically.

The results for the specular form function are shown in figures 2b and 3b. For the 0.873cm radius sphere the experimental data has some form to it and does not simply show a fixed value equivalent to the plane wave reflection coefficient. There was expected to be some reduction in value below  $x \leq 5$ , however, this is not the trend seen in the data. The non-uniformity of the small sphere response is considered to be due to the difficulty in separating the specular component, as can be seen in figure 1a, there is no time delay between the conclusion of the specular echo and the onset of surface wave radiation. However, for the case of the larger sphere there is an almost uniform response with frequency. The spectrum of the specular echo has a nominally constant value between  $x=6-28$ . There is a reduction in values at either

## SPHERE RESONANT SCATTERING

end of the spectrum and this was due to a residue in the calculations of the system's response. The prediction for  $x \geq 5$  was obtained using equation (4) which is simply defined by the reflection coefficient of the sphere in the fluid, which for the case of stainless steel spheres in water is 0.94. Although there is some variability in the data, the values for the 2.858cm sphere are close to the value for the plane reflection coefficient.

Excluding the specular signal, from the Fourier transform of the time domain signal, results in the resonant spectrum. In the small sphere case a single peak in the resonance spectrum is observed, while for the larger sphere a series is seen. The major contributions to the spectrum correspond to the Rayleigh waves and they dominate the resonant form function structure. It can be observed that the Rayleigh wave resonances have  $ka$  values which are coincidental with minima in the form function spectrum. The radiation associated with the Rayleigh waves is therefore ostensibly out of phase with the specular component for  $x \leq 18$ . Above this value the maxima in the Rayleigh resonances are not necessarily identified with the form function minima. As well as the location of the maxima being correct, it can also be seen that both the amplitude and bandwidth of the resonance peaks compare favourably with the observations. There is some discrepancy between predictions and observations within the diffraction region of the resonant spectrum for the 0.873cm sphere, and this again is thought to be due to the difficulty in separating the specular and surface wave components for this sphere. However, the results presented here show the accuracy of the resonance scattering approach in characterising the resonant component.

### 4.3 Time-Frequency

A time-frequency representation was obtained by employing a transform which started at the beginning of the time series echo. This was incrementally increased in duration with each transform to provide a description on the spectrum as it developed with time. This type of plot does not give the instantaneous frequency content with time, but shows the development with time of the spectrum. This illustrates the evolution of the form function structure as the features in the time domain signal, associated with the specular echo, and surface waves of increasing numbers of circumferential revolutions, are gradually incorporated into the transform.

An example of the experimental results for the larger sphere obtained using this approach is shown in figure 4. Three curves are presented, a) the time domain, b) the form function, and c) the time-frequency plot. In the time-frequency plot the initial echo from the specular return is seen as a broadband return representing the band limited impulse response of the sphere. Initially there is no spectral change until the second echo, principally associated with the first circumferential Rayleigh wave, is incorporated into the transform. There is immediately a change in the time-frequency plot with the uniform frequency response having a structural form due to the interference between the specular return and the Rayleigh wave radiation. Further additions of the sound radiated by repeated circumnavigations of the circumferential waves, provides the details in the spectrum. The time-frequency plot clearly illustrates the development of the spectrum and shows the trade off between the duration of the backscattered echo from the sphere which is processed and the details which are present in the spectrum. This is not due to a change in the length of the transform, all transforms have the same frequency resolution, it is the information in the transformed record which is increasing.



SPHERE RESONANT SCATTERING

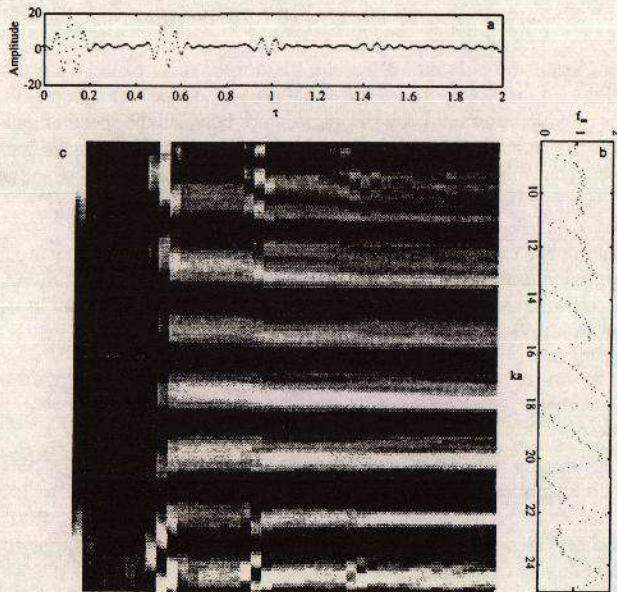


Fig.4. Measurements of the time-frequency response for the  $a=2.858\text{cm}$  sphere. a) Time series echo, b) Form function, and c) Time-frequency plot.

### 5. CONCLUSIONS

In contrast with the frequency domain, the time domain has been studied less within the framework of resonance scattering theory. One of the objectives of the present study has been to investigate this aspect of scattering and compare observations with predictions. The separation of the specularly reflected signal and the radiation due to surface wave propagation provides a time domain representation which complements the frequency domain form function representation.

The analysis in the frequency domain has covered the standard form function, the specular, and resonant form functions. The agreement between the usual  $f_n$  and prediction were comparable with other works.



# Proceedings of the Institute of Acoustics

## SPHERE RESONANT SCATTERING

The value for the specular component was generally uniform and comparable with the reflection coefficient for stainless steel in water. The resonant component, which contains the substantive information on the target again compared reasonably well with the predictions. The amplitude, location and bandwidth of the Rayleigh resonant features all corresponded favourably with predictions.

The time-frequency plots provide an insight into the development of the form function with increasing assimilation into the Fourier transform of the radiation due to repeated circumnavigations of the sphere. These transforms provide information on the interference between the specular and resonant components and how the form function develops as the length of the time series processed increases. This furnishes a representation which displays simultaneous time and frequency information, and permits the importance of the differing contributions in the time domain echo to be examined.

Lastly the application of a calibrated broadband system employing a frequency modulated signal, coupled with pulse compression techniques and Fourier analysis, can provide an effective tool for examining the scattering properties of targets. Detailed studies can be made both separately in the time and frequency domain, and also in a time-frequency regime.

## 6. ACKNOWLEDGEMENTS

We would like to thank a number of colleagues at the Applied Research Laboratory, whose support, suggestions and criticisms were valuable; Bob Rogers, Nick Chotiros, Frank Boyle and Terry Henderson. We also thank Nick Chotiros for suggesting the impulse response approach. PDT is especially grateful to Tom Muir who provided the opportunity to visit ARL. This work was supported by the Independent Research and Development Program at ARL:UT.

## 7. REFERENCES

- [1] X L BAO, C R SCHUMACHER & H UBERALL, 'Complex resonance frequencies in acoustic-wave scattering from impenetrable spheres and elongated objects', *J Acoust Soc Amer* 90(4) Pt1, 2118-2123 (1991)
- [2] R HICKLING, R K BURROWS & J F BALL, 'Rotational waves in the elastic response of spherical and cylindrical acoustic targets in water', *J Acoust Soc Amer* 89(3), 971-979 (1991)
- [3] G C GAUNAURD & M F WERBY, 'Sound scattering by resonantly excited, fluid loaded, elastic spherical shells', *J Acoust Soc Amer* 90(5) 2536-2550 (1991)
- [4] S G KARGL & P L MARSTON, 'Ray synthesis of Lamb wave contributions to the total scattering cross section for an elastic spherical shell', *J Acoust Soc Amer* 88(2) 1103-1113 (1990)
- [5] L FLAX, L R DRAGONETTE & H UBERALL, 'Theory of elastic resonance excitation by sound scattering', *J Acoust Soc Amer* 63(3) 723-731 (1978)
- [6] L FLAX, G C GAUNAURD & H UBERALL, 'The theory of resonance scattering', in *Physical Acoustics*, edited by W Mason and R Thurston. (Academic Press, New York, 1981) Vol XV Chap 3 191-194 (1981)

## SPHERE RESONANT SCATTERING

- [7] G C GAUNAURD & H UBERALL, 'RST analysis of monostatic and bistatic acoustic echoes from an elastic sphere', *J Acoust Soc Amer* 73(1) 1-12, (1983)
- [8] D BRILL & G GAUNAURD, 'Resonance theory of elastic waves ultrasonically scattered from an elastic sphere', *J Acoust Soc Amer* 81(1) 1-21 (1987)
- [9] L R DRAGONETTE, R H VOGT, L FLAX & W G NEUBAUER, 'Acoustic reflections from elastic spheres and rigid spheres and spheroids II Transient analysis', *J Acoust Soc Amer* 55(6) 1130-1137, (1974)
- [10] G MAZE & J RIPOCHE, 'Methode d'isolement et d'identification des resonances (MIIR) de cylindres et de tubes soumis a une onde acoustique plane dans l'eau', *Rev Phys Appl* 18 319-326 (1983).
- [11] M DE BILLY, 'Determination of the resonance spectrum of elastic bodies via the use of short pulses and Fourier transform theory', *J Acoust Soc Amer* 79(2) 219-221 (1986)
- [12] G QUENTIN & A CAND, 'Pulsed resonance identification method', *Elec Lett* 25(5) 353-354 (1989)
- [13] P PAREIGE, P REMBERT, J L IZBICKI, G MAZE & J RIPOCHE, 'Methode impulsionnelle numberisee (MIN) pour l'isolement et l'identification des resonances de tubes immerges', *Phys Lett A* 135(2) 143-146 (1989)
- [14] G MAZE, 'Acoustic scattering from submerged cylinders. MIIR Im/Re: Experimental and theoretical study', *J Acoust Soc Amer* 89(6) 2559-2566 (1991)
- [15] G MAZE, F LECROQ, D DECULTOT, J RIPOCHE, S K NUMRICH & H UBERALL, 'Acoustic scattering from finite cylindrical elastic objects', 90(6) 3271-3278 (1991)
- [16] M F WERBY & H B ALI, 'Time domain solution from the frequency domain: Application to resonance scattering from elastic bodies', *Computational Acoust* (Proc. 2nd 29 IMACS Symp Princeton NJ. 15-17 March 1989.) Vol 2 (Ed D Lee, A Cakmak and R Vichevetsky, Published by Elsevier Science Publishers B. V. Amsterdam, Holland) 133-148 (1990)
- [17] D BRILL, G GAUNAURD, H STRIFORS & W WERTMAN, 'Backscattering of sound pulses by elastic bodies underwater', *Appl Acoust* 33 87-107 (1991)
- [18] K L Williams & P L MARSTON, 'Backscattering from an elastic sphere: Sommerfield-Watson transformation and experimental confirmation', *J Acoust Soc Amer* 78 (3) 1093-1102 (1985)

